THE JOURNAL OF PHYSICAL CHEMISTRY C

Article

pubs.acs.org/JPCC

Optical Field Imaging of Elongated Rectangular Nanovoids in Gold Thin Film

Kohei Imura,*[,†,‡] Kosei Ueno,[‡,§] Hiroaki Misawa,[§] and Hiromi Okamoto*[,∥]

[†]Department of Chemistry and Biochemistry, School of Advanced Science and Engineering, Waseda University, Okubo, Shinjuku, Tokyo 169-8555, Japan

[‡]PRESTO, Japan Science and Technology Agency, Honcho Kawaguchi, Saitama 332-0012, Japan

[§]Research Institute for Electronic Science, Hokkaido University, Kita-Ku, Sapporo, Hokkaido 001-0021, Japan

[∥]Institute for Molecular Science and The Graduate University for Advanced Studies, Myodaiji, Okazaki 444-8585, Japan

ABSTRACT: We studied optical properties of single elongated rectangular nanovoids opened on a thin gold film by scanning near-field optical microscopy. We found that the luminescence is induced via two-photon absorption of near-infrared pulses when the sample is locally photoexcited inside the void as well as on the film. The luminescence spectrum of the void shows spectral features very similar to those observed for gold nanorods and is attributable to that from gold. On the basis of the near-field two-photon excitation imaging by detecting the luminescence, we visualized the optical fields near the voids. The optical image shows a characteristic spatial feature depending on the dimension of the void. From the close inspection of the topography and the optical images, we found that excitation probability becomes high at the metal−void boundary as well as inside the void. We found an oscillating feature along the long axis of the void. The observed spatial features were qualitatively reproduced by photonic local density-of-states based on electromagnetic calculations, and we concluded that the oscillation observed inside the void is attributed to the electromagnetic modes in the void coupled with the plasmon excitations.

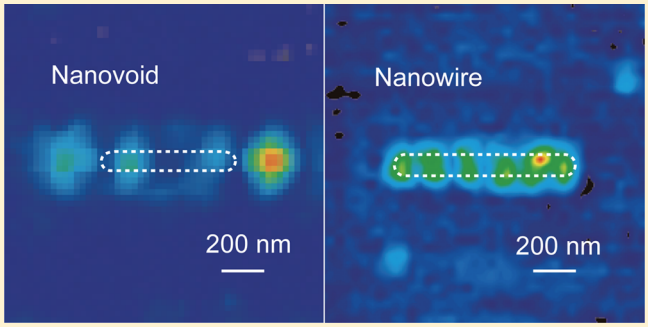

Collective oscillations of free electrons excited in metals, known as plasmons, have attracted much attention because of their ability to confine optical fields in nanometer spaces.[1−4] The confinement results in enhancement of the optical fields, with which various potential applications have been proposed.[5] It has been demonstrated in many previous studies that confined and/or enhanced optical fields are generated by suitably designed metal nanostructures. In most of those studies, with only very few exceptions, the systems investigated were metal nanostructures arranged in free spaces (particles, assemblies, and so forth in vacuum or in the air, on dielectric substrates). However, systems consisting of thin metallic films with openings of designed structures[6] (we call them hereafter voids) can also be utilized as components that construct plasmonic devices. They may create confined optical fields in the openings or in the vicinities of them, due to the excited fields extending over the metal surfaces to the surrounding areas. It is of fundamental interest to investigate the local structures of optical fields for metal voids and to compare them with those for corresponding inverted metal structures (i.e., metal particles and assemblies), as basics of nano-optics and plasmonics. The potential utility of the metal voids is also expected in various applications of the confined optical fields. For example, voids can be utilized as containers that keep various functional materials or reactants and thus yield optical devices or photochemical reaction fields in confined spaces. To create a highly confined optical field in the void, the spatial scale of the void should be sufficiently smaller than the wavelength of light. Fabrication of such a small void has become feasible recently due to the progress of the nanofabrication techniques. Optical properties of nanoslits fabricated in metallic film were reported previously, where the length of the slit was much longer than the wavelength of light and the field structures in the plane normal to the slit direction were mainly investigated.[7−11] In the present study, we focus our attention on the confined field structures in the void with a finite length along the long axis of that. The restriction of the void length may generate standing waves of plasmons in the void, which have the potential to yield enhanced optical fields in the void. Visualization of the confined optical fields in the void is the main concern of the present study.

Up to now, a number of theoretical attempts have been carried out to clarify optical field distribution in the void,[12−15] while only a very limited number of experimental observations

Special Issue: Nanostructured-Enhanced Photoenergy Conversion

Received: May 31, 2012
Revised: October 29, 2012
Published: October 30, 2012

have been reported.[16−18] Since the spatial scale of the plasmonic optical field is smaller than that of the diffraction limit of light, the microscopic method that achieves spatial resolution higher than that of a conventional optical microscope is necessary to visualize the plasmonic field. Near-field optical imaging is one of the methods to achieve that, and it has been shown that this method enables visualization of localized optical fields and surface plasmon waves in metal nanostructures.[19,20] Polarization dependence measurements of near-field imaging provide information on the direction of the electronic motion for the plasmon mode observed. Recently, it has been reported that electron microscopy with electron energy loss spectroscopic detection can also visualize plasmon modes for metal nanostructures.[21] These methods are expected to provide valuable and essential information for designing enhanced optical fields in metal nanostructures including voids.

In the present study, we visualize localized optical fields for elongated rectangular nanovoids opened on a thin gold film using near-field optical microscopy and discuss plasmonic characteristics of the nanovoids. We showed in the previous works that near-field two-photon excitation imaging is useful to visualize optical fields for gold nanostructures, where two-photon induced photoluminescence from gold is detected as a signal to construct the image.[22−24] We apply this method to the nanovoid samples. We compare the results with those of the nanowires and discuss the origin of the spatial features in the apertures.

EXPERIMENTAL SECTION

Gold nanowires and nanovoids were fabricated on coverslips using the electron beam lithography (EBL) liftoff technique. A conventional copolymer resist (ZEP-520a; Zeon Chemicals) diluted with ZEP thinner (1:1, ZEP-A; Zeon Chemicals) was spin-coated on the glass substrate (1000 rpm for 10 s and 4000 rpm for 90 s) and prebaked on a hot plate for 2 min at 180 °C. The EBL was conducted on a scanning electron microscope (SEM) (ELS-7700H; Elionix) working at an acceleration voltage of 100 kV and an electrical current of 5 pA with a dose rate of 128 μC/cm^2. After the development (ZED-N50; Zeon Chemicals) for 30 min, a gold−chromium bilayer was deposited by sputtering (MPS-4000; ULVAC) of a 2 nm chromium/40 nm gold bilayer. Liftoff was then carried out by immersion in an acetone solution for 2 min and in a resist remover solution (ZDMAC; Zeon Chemicals) for 2 min in an ultrasonic bath.

A home-built aperture-type near-field optical microscope was operated under the ambient conditions. Details of the near-field optical microscope have been reported.[19,20,25,26] The basics of the microscope are briefly described here. The apparatus consists of a light source, a sample scanner, a near-field probe, and a detection system. The aperture near-field optical probe prepared by chemical etching was purchased from JASCO Corp. The aperture size of the probe tip was determined to be 50−100 nm by SEM observation of the tip and/or near-field fluorescence images of single molecules. Optical near-field was created at the aperture by coupling the photons from a light source to the other end of the optical fiber of the near-field probe. A mode-locked Ti:sapphire laser (λ = 780−860 nm, pulse duration ca. 100 fs, repetition rate ca. 80 MHz) was used as a light source to excite two-photon luminescence from gold. The sample was illuminated through the aperture of the near-field probe. The sample substrate was installed on a closed-loop piezo-driven stage for lateral scanning. The near-field aperture was kept close to the sample surface by the shear-force feedback mechanism. The feedback signal was used for reconstructing a topographic image of the sample. Luminescence from the sample was collected by an objective lens (NA 0.9) and detected by either an avalanche photodiode (SPCM-AQR; Perkin-Elmer) or a charge-coupled device (CCD, DU-420-OE; Andor) after being dispersed by a polychromator. Polarization of the incident field was adjusted by a half- and a quarter-wave plate.

RESULTS AND DISCUSSION

Figure 1 shows the schematic view and scanning electron micrograph (SEM) images of the fabricated gold wires and

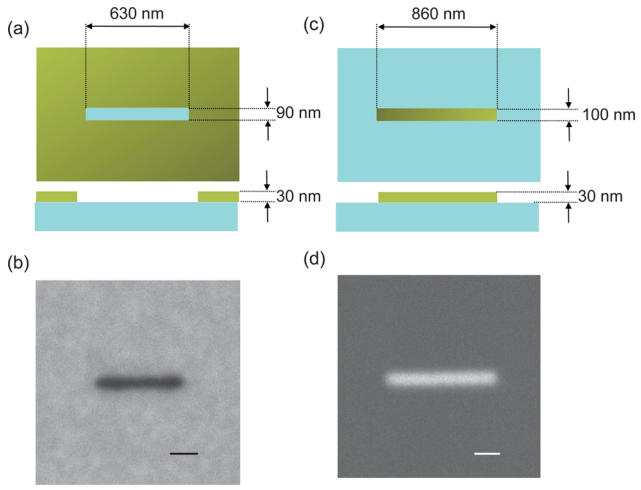

Figure 1. (a) Schematic drawing and (b) a SEM image of a nanovoid. (c) Schematic drawing and (d) a SEM image of a nanowire. Scale bars: 200 nm.

voids. From the SEM and topography images observed with the near-field microscope, the dimensions of the wires and voids were determined to be (860 ± 50) nm^l × (100 ± 10) nm^w × (30 ± 5) nm^t and (630 ± 30) nm^l × (90 ± 10) nm^w × (30 ± 5) nm^t, respectively. Both nanostructures exhibited multiple resonance peaks in the near-infrared region (at 670, 760, and 860 nm for the void and 680, 760, and 830 nm for the wire).

Two-photon-induced luminescence from gold nanostructures is effectively excited by near-infrared photons as they are resonant with the plasmons.[22−24,27−29] Figure 2(a) shows a two-photon-induced luminescence spectrum of the void sample. The sample nanovoid was locally excited at a position inside the void, and even in this case luminescence emitted from the sample was observed. Since either the metal or luminescent material is absent from the excited volume inside the void, luminescence must be radiated from the outside of the void. The observed luminescence spectrum shows a shoulder near 550 nm and a peak near 650 nm. The spectral features are very similar to those observed for a chemically synthesized gold nanorod (20 nm$^\phi$ × 550 nm^l) as shown in Figure 2(b). The photon energies of the shoulder (~18 000 cm^{-1}) and the peak (~15 000 cm^{-1}) are in good agreement with the energy gaps between the Fermi level and the d-band near the L symmetry point and that near the X point, respectively. On the basis of these findings, we concluded that the luminescence is arising from gold. The luminescence is induced by the local excitation of an electromagnetic mode in the void, which excites the collective oscillation of electrons in the gold film. This result

dx.doi.org/10.1021/jp305343g | J. Phys. Chem. C 2013, 117, 2449−2454

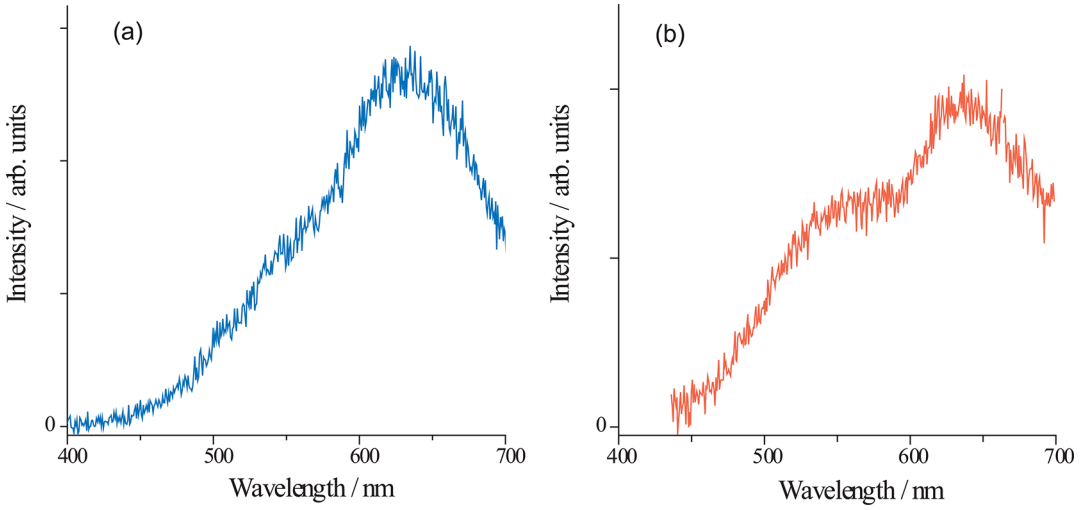

Figure 2. Two-photon luminescence spectra of (a) a nanovoid (630 $nm^l \times 90$ $nm^w \times 30$ nm^t) and (b) a gold nanorod (diameter ca. 20 $nm^\varphi \times 550$ nm^l), respectively.

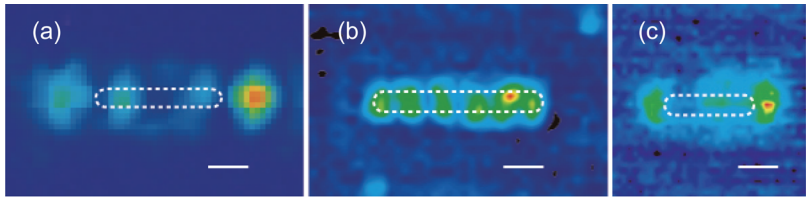

Figure 3. Two-photon excitation images of (a) a nanovoid (630 $nm^l \times 90$ $nm^w \times 30$ nm^t), (b) a nanowire (860 $nm^l \times 100$ $nm^w \times 30$ nm^t), and (c) a nanovoid (450 $nm^l \times 100$ $nm^w \times 30$ nm^t). Dotted lines indicate the approximate shapes of the structures. Excitation wavelength: 810 nm for (a), 800 nm for (b), and 800 nm for (c). Scale bars: 200 nm.

indicates that the spatial coherence of the mode extends over the excitation volume, i.e., to the metallic part. The emission of photons probably takes place predominantly at the gold film−void boundary.

Figure 3(a,b) shows near-field two-photon excitation images observed for a void (630 $nm^l \times 90$ $nm^w \times 30$ nm^t) and a wire (860 $nm^l \times 100$ $nm^w \times 30$ nm^t), respectively. Excitation wavelengths for the void and the wire were 810 and 800 nm, respectively. In both cases, the incident field was polarized along the long axis of the nanostructures. In the case of the wire, a periodic oscillation pattern was observed along the long axis of the wire. The oscillation period is about 160 ± 20 nm, which is of similar value with that observed for chemically synthesized gold nanorods with a diameter of 30 nm.[20,30] In a similar manner, an oscillation feature along the long axis was observed for the void as seen in Figure 3(a). Each void showed four bright spots. From the close inspection of the image, we found that two of the four bright spots were located outside of the void near the end edges, and the other two were inside the void. The distance between the two spots in the void was 350−400 nm, which was longer than the period for the wire.

It has been well established that the observed oscillation feature in the wire is attributed to a longitudinal plasmon mode resonantly excited by the incident photons, based on the dispersion relation of the plasmon.[31] Although the period of the oscillation observed for the void and the wire is different from each other, the feature for the void in Figure 3(a) looks similar to that observed for the wire in that the signal is spatially oscillating along the long axis of the structure. This observation suggests that the features are of similar origin. That is, in both nanowires and nanovoids, resonant standing-wave plasmons were generated due to the boundary condition for the finite-length pseudo one-dimensional structure, and the square moduli of the waves were visualized in the near-field images. We discuss here in detail the origin of the oscillatory feature in the void. Void length dependence of the oscillation feature is supportive to clarify the origin of the oscillation inside the void. We thus recorded a two-photon excitation image of a shorter nanovoid (450 $nm^l \times 100$ $nm^w \times 30$ nm^t) as shown in Figure 3(c). The observed image showed a similar spatial feature observed in Figure 3(a). We found three bright spots for each void, one spot in the void and the other two outside the void on the metallic film near the end edges. Fewer spots were found in the void as the void length became shorter. This result implies that the standing wave is generated in the void, and the spot corresponds to the antinodes of the waves. The number of the spots in the void varies as the length of the void changes because the number of the antinodes in the wave is determined by the boundary condition of the system. The observed void-length dependence of the number of the bright spots in the void shows a qualitative analogy to that observed for the wire. This result strongly suggests that the spatial feature observed is attributed to the plasmon mode resonantly excited in the void.

To get further support for the interpretation above, we have made a simulation of the near-field image based on the electromagnetic theory. It has been discussed in many works that calculation of photonic local density-of-states (LDOS) is helpful for interpretation of the physical origin of the near-field images.[19,20,32] Photonic LDOS can be calculated by the Green dyadic methods based on the Maxwell equations.[33,34] Photonic LDOS at a position $\mathbf{r}$ and a frequency ω is defined, using the

dx.doi.org/10.1021/jp305343g | J. Phys. Chem. C 2013, 117, 2449−2454

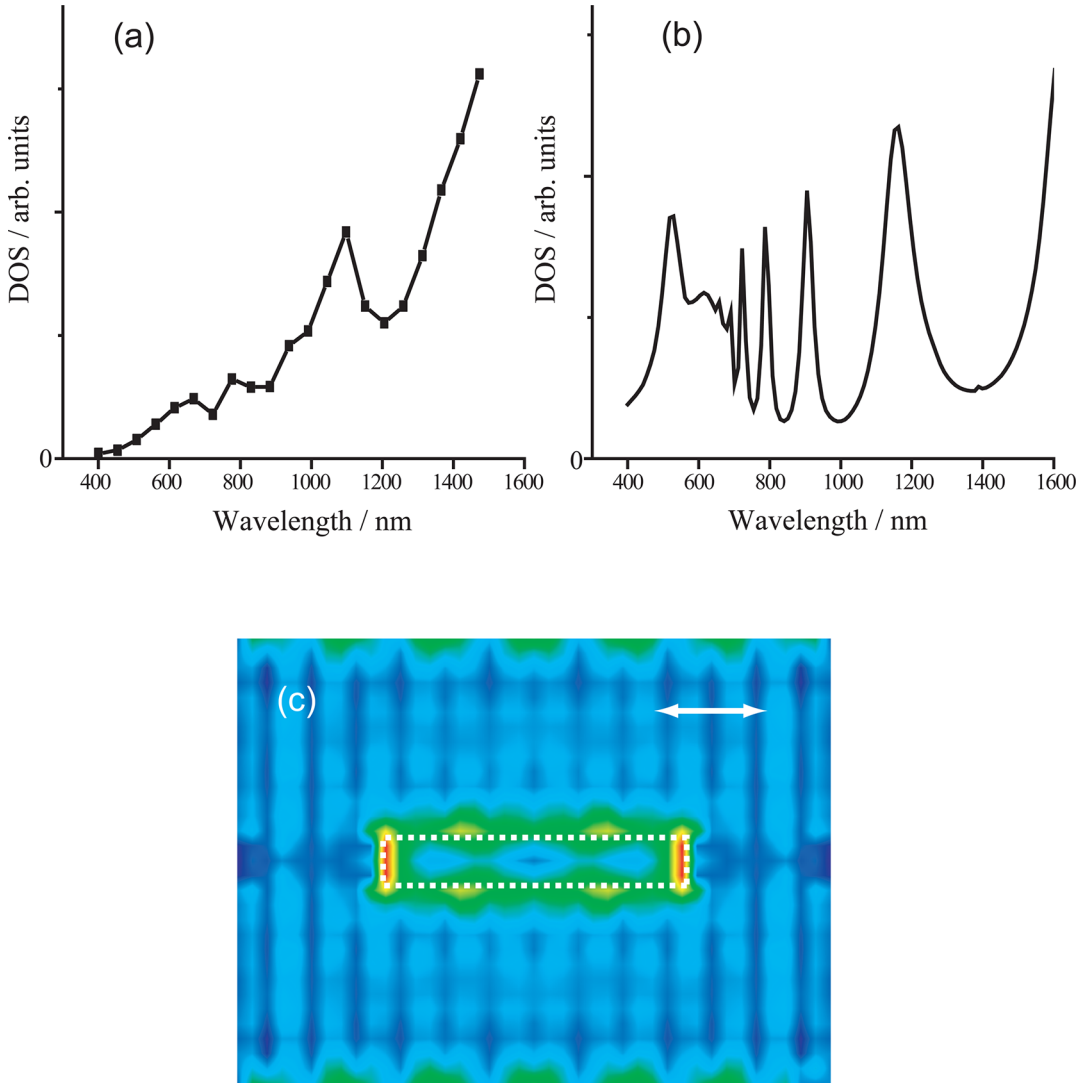

Figure 4. Calculated density-of-states spectra of (a) a nanovoid (630 $nm^l \times 90$ $nm^w \times 30$ nm^t) and (b) a nanowire (600 $nm^l \times 30$ $nm^w \times 30$ nm^t), respectively. (c) Local density-of-states map of the nanovoid calculated at 786 nm. Dotted square indicates the shape of the void. Arrow indicates the direction of polarization.

complete set of orthogonal electromagnetic eigen functions ϕ_n of the system, as

$$\rho(\mathbf{r}, \omega) = \sum \delta(\omega - \omega_n)\phi_n(\mathbf{r})\phi_n^*(\mathbf{r})$$

where ω_n represents resonance frequency of the n-th eigen mode. We calculated the LDOS map for the area in the neighbor of the void, following the procedures reported by Girard and co-workers.[33] In this study, we assumed that the sample is surrounded by a homogeneous medium to simplify the calculation. For more rigorous treatment, the presence of the sample substrate and an adhesive layer beneath the gold film has to be taken into account in the calculation. The influence of the layered system on the optical properties of the sample was discussed in some reports.[35,36] The nanovoid structure was discretized into cubic cells, and a polarization component along the long axis of the structure was obtained. The size of the calculation area was 1230 $nm^l \times 930$ $nm^w \times 45$ nm^h. The refractive index of the surrounding medium used for the calculation was 1.5. Photonic LDOS in the plane 15 nm above the structure was calculated. Since the model was approximated as a scattering system with a simple geometry and the calculation area was limited to a finite size, the results of simulation may be useful only for qualitative purposes. The electromagnetic density-of-states (DOS) at a frequency ω was estimated by integrating $\rho(\mathbf{r},\omega)$ over the area covering the void and is plotted as a function of the wavelength ($\lambda = 2\pi c/\omega$) in Figure 4(a). We found that the calculated DOS spectrum depends a little on the integration area in the void, but the dependence is not serious for our qualitative purposes. In the calculated DOS spectrum, several resonance peaks are found. These resonances show a propensity similar to that of a gold wire (Figure 4(b)). Namely, the DOS spectrum shows several resonance peaks, and the resonance peak intensity becomes higher in the longer-wavelength region. The similarity between the DOS spectra of the void and the wire indicates that the resonances in the void originate from surface-plasmon excitations near the boundary area of the void. In far-field transmission spectra of circular and rectangular voids, resonance peaks were observed and were assigned to plasmon resonances.[6,17] These observations are consistent with the appearance of the resonance peaks in the calculated DOS spectrum.

dx.doi.org/10.1021/jp305343g | J. Phys. Chem. C 2013, 117, 2449−2454

Figure 4(c) shows the calculated LDOS map in the neighbor of the void. We found from the simulations that the spatial feature of LDOS depends strongly on the oscillation frequency and the direction of polarization. In Figure 4(c), the calculated LDOS polarized along the long axis of the void is plotted to facilitate comparison with the observed near-field image. The calculated image shows LDOS concentrated around the metal−void interface, and the highest intensity is found at the end-edges of the void. The LDOS profile is not homogeneous inside the void, and an oscillating feature is visible along the long axis of the void. Locations showing high LDOS are qualitatively in good agreement with the positions of bright spots in the observed near-field image. This finding is reasonable considering the general tendency that the local optical excitation probability is roughly proportional to the LDOS.[31] In the metallic film part outside the void, on the other hand, the calculated LDOS shows poor agreement with the observed near-field image. We found that LDOS calculated at a shorter wavelength (~743 nm) is enhanced near the end edges outside the void and that the locations of the enhanced LDOS in this case agree with those of the bright spots observed in the near-field image. It should be noticed here that the void geometry for the calculation did not exactly coincide with that for the experimental observation. For example, the corners of the void were rectangular in the calculation but were rounded in the experimental specimen. In principle, the geometry of the void may be reproduced using the finely discretized cells. In that case, however, the size of the cell must be smaller, and the number of the cells becomes extremely large. Such a calculation is computationally very demanding and is beyond the scope of our analysis. The change of the corner shape varies the resonance condition and the spatial features of LDOS. In general, rounding of the corners of noble metal nanostructures yields blue-shifts of plasmon resonances.[37] From these considerations, the bright spots observed in the metallic film part outside the void are ascribed to the plasmon-induced LDOS enhancements.

Finally, we mention the relation between findings in the present study and the Babinet's principle in optics. The simple version of Babinet's principle (scalar wave theory) tells us that the spatial distribution of waves scattered by a screen (screen I) and that by a screen of a complementary geometry (screen II) coincide with each other. The screens are assumed here to be made of infinitesimally thin perfect conductors. The wire and the void structures studied here can be regarded as geometries roughly complementary to each other in their qualitative nature, while thicknesses of the structures are not negligible. In the present study, both the wire and the void gave spatially oscillating optical field distributions. In this regard, the characteristic features observed in the near-field images are similar to each other, and it looks as if this result is relevant to the Babinet's principle. However, it should be noted that optical fields are actually vector fields that consist of mutually correlated electric and magnetic fields, and hence the rigorous vector theory of Babinet's principle should be adopted for optical phenomena. Under the vector theory of Babinet's principle, the distribution of the electric-field waves scattered by screen I coincides with that of the *magnetic-field waves* scattered by screen II. What we experimentally observed in optical measurements were, however, electric fields for both screens I and II. Therefore, the results obtained in the present study cannot be explained simply by the Babinet's principle. We previously drew the same conclusion for the other complementary systems, i.e., assemblies of disks and voids.[18] To discuss the relation between the near-field images and the Babinet's principle, further studies based on polarization-dependent near-field measurements for wires and voids with various geometries are necessary, as well as theoretical analyses.

In summary, we performed near-field two-photon excitation imaging of nanovoids opened on gold thin films to visualize the optical fields. We found that the optical fields were confined at metal edges near the void as well as inside the void. Inside the void, the optical fields exhibited spatial oscillation along the long axis. With the aid of the electromagnetic LDOS calculations, the oscillating feature was attributed to the electromagnetic modes in the void coupled with the plasmon excitations.

AUTHOR INFORMATION

Corresponding Author

*E-mail: imura@waseda.jp; aho@ims.ac.jp.

Notes

The authors declare no competing financial interest.

ACKNOWLEDGMENTS

This work was supported by Asahi foundation, Research Foundation for Opto-Science and Technology, Iketani Science and Technology Foundation, Grants-in-Aid for Scientific Research (Grant Nos. 18205004, 18685003, 19049001, 19049015, 22225002, 24655020, and 24350014) from the Japan Society for the Promotion of Science and from the Ministry of Education, Culture, Sports, Science and Technology, and a Grant-in-Aid from Hokkaido Innovation through Nanotechnology Support (HINTS).

REFERENCES

(1) Kreibig, U.; Vollmer, M. *Optical Properties of Metal Clusters*; Springer-Verlag: Berlin, 1995.
(2) Barnes, W. L.; Dereux, A.; Ebbesen, T. W. *Nature* **2003**, *424*, 824−830.
(3) Kelly, K. L.; Coronado, E.; Zhao, L. L.; Schatz, G. C. *J. Phys. Chem. B* **2003**, *107*, 668−677.
(4) Imura, K.; Ueno, K.; Misawa, H.; Okamoto, H. *Nano Lett.* **2011**, *11*, 960−965.
(5) Stockman, M. I. *Opt. Express* **2011**, *19*, 22029−22106.
(6) Genet, C.; Ebbessen, T. W. *Nature* **2007**, *445*, 39−46.
(7) Wei, P. −K.; Chou, H.-L.; Fann, W.-S. *Opt. Express* **2002**, *10*, 1418−1424.
(8) Wei, P. −K.; Chou, Cheng, Y.-R.; Wei, C.-H.; H.-L.; Fann, W.; Tegenfeldt, J. O. *Opt. Commun.* **2005**, *253*, 198−204.
(9) Seo, M. A.; Adam, A. J.; Kang, J. H.; Lee, J. W.; Jeoung, S. C.; Park, Q. H.; Planken, P. C.; Kim, D. S. *Opt. Express* **2007**, *15*, 11781−117789.
(10) Aigouy, L.; Lalanne, P.; Liu, H.; Julié, G.; Mathet, V.; Mortier, M. *Appl. Opt.* **2007**, *46*, 8573−8577.
(11) Kihm, H.-W.; Kim, Q. H.; Kim, D. S.; Ahn, K. J.; Kang, J. H. *Opt. Express* **2010**, *18*, 15725−15731.
(12) Bethe, H. A. *Phys. Rev.* **1944**, *66*, 163−182.
(13) Chang, S.-H.; Gray, S. K. *Opt. Express* **2005**, *13*, 3150−3165.
(14) Grosjean, T.; Ibrahim, I. A.; Suarez, M. A.; Burr, G. W.; Mivelle, M.; Charraut, D. *Opt. Express* **2010**, *18*, 5809−5824.
(15) Popov, E.; Bonod, N.; Nevière, M.; Rigneaut, H.; Lenne, P.-F.; Chaumet, P. *Appl. Opt.* **2005**, *44*, 2332−2337.
(16) Yin, L.; Vlasko-Vlasov, V. K.; Rydh, A.; Pearson, J.; Welp, U.; Chang, S.-H.; Gray, S. K.; Brown, D. B.; Kimball, C. W. *Appl. Phys. Lett.* **2004**, *85*, 467−469.
(17) Degiron, A.; Lezex, H. J.; Yamamoto, N.; Ebbesen, T. W. *Opt. Commun.* **2004**, *239*, 61−66.

(18) Kim, S. I.; Imura, K.; Kim, S.; Okamoto, H. *J. Phys. Chem. C* **2011**, *115*, 1548−1555.
(19) Okamoto, H.; Imura, K. *Prog. Surf. Sci.* **2009**, *84*, 199−229.
(20) Imura, K.; Okamoto, H. *Bull. Chem. Soc. Jpn.* **2008**, *81*, 659−675.
(21) Nelayah, J.; Kociak, M.; Stéphan, O.; García de Abajo, F. J.; Tencé, M.; Henrard, L.; Taverna, D.; Pastoriza-Santos, I.; Liz-Marzán, L. M.; Colliex, C. *Nature Phys.* **2007**, *3*, 348−353.
(22) Imura, K.; Nagahara, T.; Okamoto, H. *J. Am. Chem. Soc.* **2004**, *126*, 12730−12731.
(23) Imura, K.; Nagahara, T.; Okamoto, H. *J. Phys. Chem. B* **2005**, *109*, 13214−13220.
(24) Imura, K.; Nagahara, T.; Okamoto, H. *Appl. Phys. Lett.* **2006**, *88*, 023104.
(25) Imura, K.; Okamoto, H. *Progress in Nanophotonics I*; Ohtsu, M., Ed.; Springer-Verlag: New York, 2011; pp 127−160.
(26) Okamoto, H.; Imura, K. *Advances in Multi-Photon Processes and Spectroscopy*; Lin, S. H., Villaeys, A. A., Fujimura, Y., Eds.; World Scientific: New Jersey, 2011; pp 175−209.
(27) Boyd, G. T.; Yu, Z. H.; Shen, Y. R. *Phys. Rev.* **1986**, *33*, 7923−7936.
(28) Schuck, P. J.; Fromm, D. P.; Sundaramurthy, A.; Kino, G. S.; Moerner, W. E. *Phys. Rev. Lett.* **2005**, *94*, 017402.
(29) Farrer, R. A.; Butterfield, F. L.; Chen, V. W.; Fourkas, J. T. *Nano Lett.* **2005**, *5*, 1139−1142.
(30) Schider, G.; Krenn, J. R.; Hohenau, A.; Ditlbacher, H.; Leitner, A.; Aussenegg, F. R. *Phys. Rev. B* **2003**, *68*, 155427.
(31) Imura, K.; Nagahara, T.; Okamoto, H. *J. Chem. Phys.* **2005**, *122*, 154701.
(32) Chicanne, C.; David, T.; Quidant, R.; Weeber, J. C.; Lacroute, Y.; Bourillot, E.; Dereux, A.; Colas des Francs, G.; Girard, C. *Phys. Rev. Lett.* **2002**, *88*, 097402.
(33) Girard, C.; Dereux, A. *Rep. Prog. Phys.* **1996**, *59*, 657−699.
(34) Greffet, J.-J.; Carminati, R. *Prog. Sur. Sci.* **1997**, *56*, 133−237.
(35) Paulus, M.; Gay-Balmaz, P.; Martin, O. J. F. *Phys. Rev. E* **2000**, *62*, 5767−5776.
(36) Colas des Francs, G.; Molenda, D.; Fischer, U. C.; Naber, A. *Phys. Rev. B* **2005**, *72*, 165111.
(37) Wiley, B. J.; Im, S. H.; Li, Z.-Y.; McLellan, J.; Siekkinen, A.; Xia, Y. *J. Phys. Chem. B* **2006**, *110*, 15666−15675.